ACS APPLIED MATERIALS & INTERFACES

Research Article

www.acsami.org

Interfacial Microstructure and Properties of Carbon Fiber Composites Modified with Graphene Oxide

Xiaoqing Zhang, Xinyu Fan,* Chun Yan, Hongzhou Li, Yingdan Zhu, Xiaotuo Li, and Liping Yu

Ningbo Key Laboratory of Polymer Material, Ningbo Institute of Material Technology and Engineering, Chinese Academy of Sciences, Ningbo 315201, China

Supporting Information

ABSTRACT: The performance of carbon fiber-reinforced composites is dependent to a great extent on the properties of fiber−matrix interface. To improve the interfacial properties in carbon fiber/epoxy composites, we directly introduced graphene oxide (GO) sheets dispersed in the fiber sizing onto the surface of individual carbon fibers. The applied graphite oxide, which could be exfoliated to single-layer GO sheets, was verified by atomic force microscope (AFM). The surface topography of modified carbon fibers and the distribution of GO sheets in the interfacial region of carbon fibers were detected by scanning electron microscopy (SEM). The interfacial properties between carbon fiber and matrix were investigated by microbond test and three-point short beam shear test. The tensile properties of unidirectional (UD) composites were investigated in accordance with ASTM standards. The results of the tests reveal an improved interfacial and tensile properties in GO-modified carbon fiber composites. Furthermore, significant enhancement of interfacial shear strength (IFSS), interlaminar shear strength (ILSS), and tensile properties was achieved in the composites when only 5 wt % of GO sheets introduced in the fiber sizing. This means that an alternative method for improving the interfacial and tensile properties of carbon fiber composites by controlling the fiber−matrix interface was developed. Such multiscale reinforced composites show great potential with their improved mechanical performance to be likely applied in the aerospace and automotive industries.

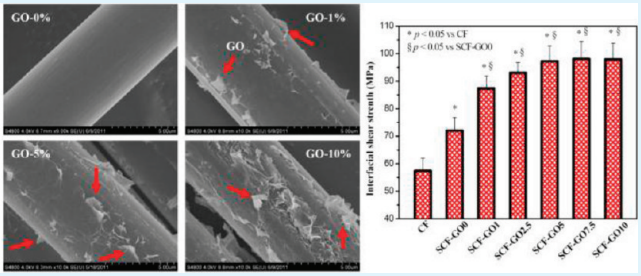

KEYWORDS: *graphene, interfacial microstructure, interfacial properties, carbon fiber, fiber sizing, composites*

1. INTRODUCTION

Carbon-fiber-reinforced composites with their favorable strength-to-weight and stiffness-to-weight ratios are replacing their metal counterparts in a variety of high-performance structural applications,[1,2] such as for aerospace and automotive, industries. However, the performance of fiber-reinforced composites is, to a large extent, controlled by the properties of fiber−matrix interface. Good interfacial properties are essential to ensure efficient load transfer from matrix to fillers, which helps to reduce stress concentrations and improves overall mechanical properties. Consequently, there is great interest in developing new concepts for improving the strength of carbon fiber−matrix interface.

In recent years, it has been demonstrated that the addition of graphenes in the matrix can increase the toughness of the matrix and improve the interfacial properties of graphene based composites.[3−6] Furthermore, multiscale reinforcement, containing fibers together with graphenes in the matrix or on the surface of the fibers, can enhance the interface properties (e.g., fatigue life) of fiber reinforced composites.[7] In ref 7, graphenes were introduced into the glass-fiber/epoxy composites by two methods: (1) infiltrating into the epoxy resin matrix and (2) directly spraying graphenes onto the glass fibers (E-glass woven fabric plies) prior to curing the composites. It was observed that the number of cycles to failure for the case of graphenes directly spray-coated onto the glass fibers was about 8 times greater than when the graphenes were uniformly dispersed in the resin. It has been concluded that the micrometer size dimensions, high aspect ratio, and two-dimensional sheet geometry of graphene make it highly effective at deflecting cracks in bending/shear when placing them right at the micro fiber−matrix interface of composites.

However, regardless of the potential use of nanofillers in the fiber sizing, it received very limited attention in the literature. Yang et al.[8] used the nano-SiO_2-modified epoxy sizing to coat carbon fibers, and then investigated the interfacial shear strength (IFSS) and the interlaminar shear strength (ILSS) of the carbon fibers in the epoxy by means of the single fiber-composite fragmentation test and three-point short beam shear test, respectively. The test indicated a 39% improvement of IFSS and a 16% improvement of ILSS for the nano-SiO_2 modified epoxy sizing treated carbon fiber in comparison with the unsized fibers in carbon/epoxy composites. Mader et al.[9−12] described an online process by which a nanometer-scale hybrid coating layer based polymer with low fraction of single or multiwalled carbon nanotubes (SWCNTs, MWCNTs) and/or

Received: December 12, 2011
Accepted: March 5, 2012
Published: March 5, 2012

nanoclays, as mechanical enhancement, is applied to glass fibers. The results indicated that the nanostructured and functionalized glass fibers show significantly improved tensile strength and interfacial shear strength. Godara et al.[13,14] reported over 90% improvement of IFSS in a glass-fiber/epoxy composites when CNTs were introduced solely in the fiber sizing where the IFSS was evaluated using a single-fiber push-out microindentation. In ref 13, the glass fibers were directly coated with epoxy-compatible phenoxy-based sizing containing MWCNT without removal of the commercial sizing. However, the effect of epoxy-compatible phenoxy-based sizing on the IFSS improvement in the system was not considered. To the best of our knowledge, there are large numbers of studies in the literature reporting the increase in IFSS due to the fiber sizing.[15−17] Thus, it is necessary to study the extent of IFSS improvement due to separate effects of nanofillers and fiber sizing.

In the present work, we explored an alternative method for the fabrication of multiscale composites, and studied the effect of graphene oxide (GO) and the microstructure of carbon−fiber interface on the interfacial performance of carbon fiber-reinforced composites. The GO was dispersed in the fiber sizing and then was directly placed on the surface of individual carbon fiber. This route takes advantage of the developed techniques for the dispersion of GO in resin, and makes it possible to scale up from research laboratory to industrial applications. The carbon fiber surface topography was examined by scanning electron microscopy (SEM). The distribution of GO sheets in the sizing resin surrounding the carbon fiber was detected by SEM after removing the sizing resin by thermal defunctionalization in N_2 atmosphere. The interface properties between carbon fibers and resin matrix in composites were evaluated by microbond test and three-point short beam shear test. The tensile properties of unidirectional (UD) GO-modified carbon fiber composites were tested in the fiber direction by using universal mechanical machine.

2. EXPERIMENTAL SECTION

2.1.1. Materials. *Raw Materials.* Commercially available T700S carbon-fibers (12K, 1.80 g/cm^3), with an average diameter of 7 μm, purchased from Japan Toray, were used as reinforcing fillers in the present work. The matrix was composed of a mixture of E-20 and E-54 epoxy resin, which were obtained from Yueyang chemical Co. Ltd., China. The hardener includes 4,4′-diaminodiphenylmethane (DDM), 4,4′-diaminodiphenylsulfone (DDS) and 2-Ethyl-4-methylimidazole. Natural graphite flakes with an average diameter of 10 μm were supplied from Haida Graphite Factory (Qingdao, China). Concentrated sulfuric acid (95−98%), concentrated nitric acid (68%) and hydrochloric acid (36−38%) were purchased from Shanghai Chemical Factory, China. $KMnO_4$ was obtained from Sinopharm Chemical reagent Co., Ltd. (Shanghai, China). An epoxy emulsion (NEOXIL 965) with solid contents of 52−56 wt % was kindly supplied by DSM (China) Ltd. as fiber sizing resin.

2.1.2. Preparation of Graphene Oxide (GO). GO was prepared using a modified Hummers and Offeman's method.[18,19] In a typical procedure, 5 g of graphite, 5 g of $NaNO_3$, and 200 mL of H_2SO_4 were stirred together in an ice bath for 15 min below 5 °C. Twenty grams of $KMnO_4$ was slowly added into the mixture while stirring, and the rate of addition was controlled to prevent the mixture temperature from exceeding 20 °C. The mixture was then transferred to a 30 °C water bath and stirred for about 30 min, forming a thick paste. Subsequently, 200 mL deionized water was added dropwise into the mixture with strong mechanical stirring and the temperature was controlled below 98 °C. After 15 min, the mixture was further treated with 700 mL of deionized water and 60 mL of 30% H_2O_2 solution. The warm solution was then filtered and subjected to cycles of washing with deionized water until the pH value of supernatant reached 6. Graphite oxide suspension was stored in a seal bottle. To obtain graphene oxide, we diluted the resulting graphite oxide suspension with deionized water, sonicated it for 1 h, and then centrifuged it at 7000 rpm for 15 min to remove the unexfoliated graphite oxide. The homogeneous aqueous dispersions of graphene oxide with concentration up to 5 mg/mL were readily obtained by removing part of water through rotation evaporation, which was then used to prepare GO-modified sizing.

2.1.3. Introduction of Graphene Oxide (GO) on the Carbon Fibers. Before introduction of GO on the carbon fibers, the flowing steps are necessary:

(1) To exclude the possible effects of commercial sizing from the IFSS improvement in the system, we first refluxed the commercial carbon fibers (T700S) in acetone for 48 h to remove the commercial sizing before being used.

(2) The aqueous dispersion of graphene oxide (5 mg/mL) were added into epoxy emulsions with GO contents of 0, 1, 2.5, 5, 7.5 wt, and 10 wt %, and the mixture was stirred for 15 min, followed by diluted with deionized water to make a final concentration of 1.5 wt % of sizing resin (containing GO). In this work, the sizing resin was kept constantly at 1.5 wt % in the fiber sizing, and the GO sheets vary from 0 to 10 part per hundred of sizing resin.

(3) The virgin carbon fibers were pulled through the GO-modified sizing and by subsequent drying them at 100 °C. The extraction speed was maintained slow enough to achieve good wetting of the fibers and to allow the excess resin to be removed. All necessary precautions were taken to prevent any damage during handling of the fibers. Finally, these GO-modified carbon fibers were stored in dryer before being used.

2.2. Sample Preparation for Microbond Test. For the further investigation of interfacial properties between the fiber and the matrix resin, we carried out a microbond test to determine the interfacial shear strength (IFSS) of the carbon fiber/epoxy resin composite. The specimens of microbond test were prepared in paper frames with dimension of 26 mm × 58 mm. The free fiber length was approximately 30 mm. Some epoxy resin droplets were placed against a monofilament and cured (Figure 1A). The cure procedure of the epoxy resin droplets was used as follows: heating from 25 to 90 °C for 7 min; holding at 90 °C for 1.5 h; heating from 90 to 120 °C for 3 min; holding at 120 °C for 2 h; then cooling to room temperature naturally.

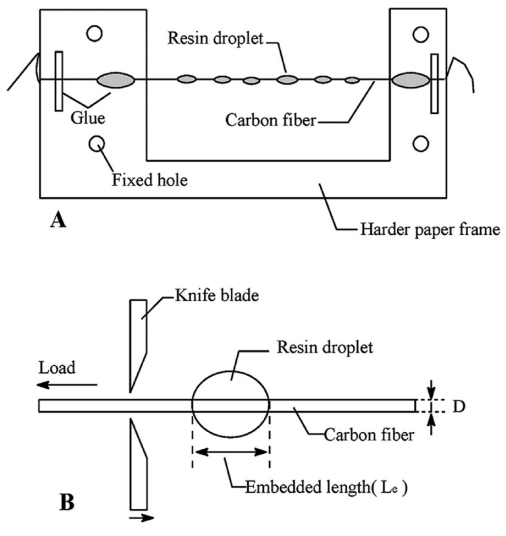

Figure 1. Schematic illustration of microbond test, not to scale.

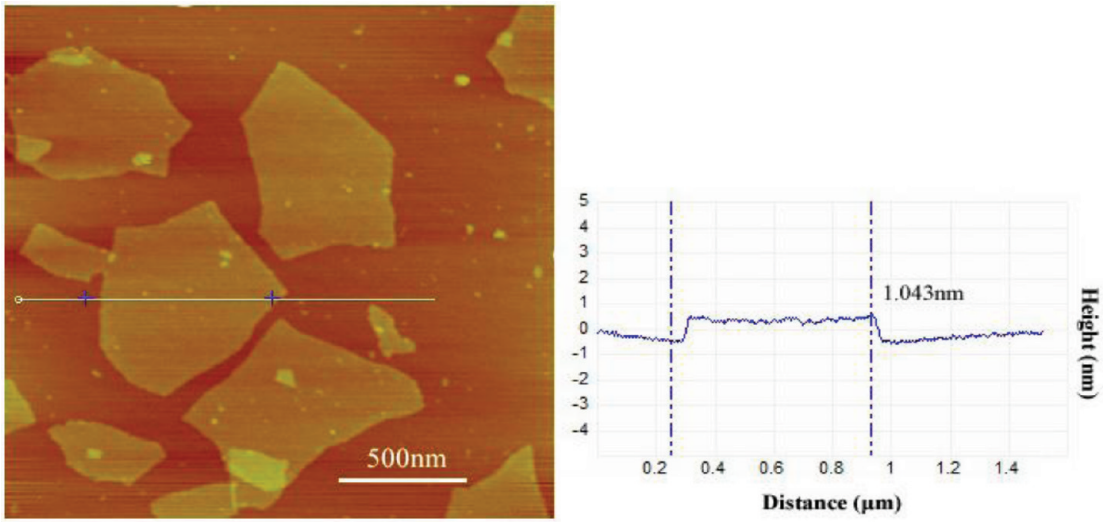

Figure 2. AFM image (left) of graphene oxide sheets dispersion in water on freshly cleaved mica surface through drop-casting, and height profile (right) along the white line indicating a sheet thickness of ~1 nm.

2.3. Sample Preparation for Three-Point Short Beam Shear Test and Tensile Test. Preparation of the unidirectional (UD) carbon fiber composites was done following the protocol: (1) Carbon fibers were impregnated using an acetone solution of epoxy resin (E-20 and E-54 in a weight ratio of 60: 40) with 20 wt % hardener (a mixture of DDM, DDS and 2-Ethyl-4-methylimidazole in a weight ratio of 10:40:1.5) for manufacturing prepregs. (2) Once the prepregs were prepared, they were cut into sheets, and then put them into vacuum oven at 30 °C for 12 h to remove residual acetone. (3) To produce a unidirectional composite plate, we laid up prepreg sheets in the unidirectional fiber orientation and cured them at 90 °C for 1.5 h followed by a post-curing step at 120 °C for 2 h. The laminates were produced in an autoclave at vacuum of −0.08 to −0.09 MPa, in a vacuum bag using peel-ply and bleeder. Composite laminates were obtained with the final fiber volume fraction in the range from 45 to 50%. The laminate plates with dimensions of 150 mm × 150 mm were prepared for the three-point short beam shear test. The laminate plates with dimensions of 300 mm × 300 mm were prepared for the tensile test.

2.4. Characterizations. Atomic force microscope (AFM) observation of GO sheets was performed on a DI Multimode V scanning probe microscope (Dimension3100 V, Veeco, USA). The GO sheets were dispersed in water and dip-coated onto freshly cleaved mica surfaces before testing. The scanning electron microscopy (SEM) images of the carbon fibers were obtained on a Hitachi S-4800 field-emission SEM system (operated at 4 kV). The samples were coated with Pt/Au by sputtering.

A microbond test was carried out using an interfacial microbond evaluation instrument (Model HM410) made by Tohei Sanyon Corporation of Japan (Figure 1B). The illustration of microbond test was shown in Figure 1. The fiber was loaded at a speed of 1 μm/s from the matrix while the force was recorded against the displacement using a computer. The interfacial shear strength, τ, was determined using the following equation[20]

$$\tau = \frac{F_{max}}{\pi D L_e} \quad (1)$$

where F_{max} is the force at the moment when the interfacial debonding or sliding occurs, D is the carbon fiber diameter, and L_e is the embedded length of carbon fiber in the epoxy resin droplet. A variation of the embedded lengths in a range of 70−100 μm was allowed for test. At least 50 valid data were collected for every type carbon fiber, and then averaged. Student's t test was used to compare differences for the quantitative variables, with significance assigned at $p < 0.05$.

The three-point short beam shear test was carried out to determine the effect of GO modified sizing on the interlaminar shear strength (ILSS) of the unidirectional carbon fiber composites, according to the ASTM D-2344 standards.[21] The dimensions of carbon fiber composite specimens for three-point short beam shear tests were: 12.0 mm length, 4.0 mm width, and 2.0 mm thickness. The tests were performed in an Instron mechanical testing machine (Instron5567, USA) using a cross-head speed of 1 mm/min. The interlaminar shear strength (ILSS) was calculated with the following formula[21]

$$\mathrm{ILSS} = \frac{0.75P}{bh} \quad (2)$$

where P is the failure load and b and h are the specimen width and thickness, respectively. A minimum of 10 specimens were tested for each type of composites. The obtained results are quoted as the average values with deviation from all tested samples of each composite. Student's t test was used to compare differences for the quantitative variables, with significance assigned at $p < 0.05$.

The tensile test of UD carbon fiber composites were performed by using an Instron5985 machine, according to ASTM D3039, with a cross-head speed of 2 mm/min and a load cell of 250 kN. The specimens were cut to size of 250 mm × 15 mm × 1.0 mm with four end-tabs bonded to both ends (aluminum tab with dimensions of 50 mm × 15 mm × 1.0 mm). At least five specimens were tested for each type of composites. The obtained results are quoted as the average values with deviation from all tested specimens of each material. Student's t test was used to compare differences for the quantitative variables, with significance assigned at $p < 0.05$.

3. RESULT AND DISCUSSION

3.1. Exfoliation of Graphite Oxide in Water. Because of the hydrophilic nature of the oxygenated graphene layers, it is easy to exfoliate the graphite oxide layers in aqueous media by ultrasonic treatment. To investigate the degree of the exfoliation of the graphite oxide in water, atomic force microscopy (AFM) imaging of graphene oxide (GO) sheets dispersion in water after their deposition on a freshly cleaved mica sheet through drop-casting was carried out. A representative AFM image of GO sheets is shown in Figure 2, which reveals the presence of irregularly shaped sheets with uniform thickness and the size of GO sheets mainly covers 0.5−2 μm. As indicated in Figure 2 for the part marked by the white line, the thickness of the sheets is typically 1.0 nm, which is in good agreement with previous reported single-layer

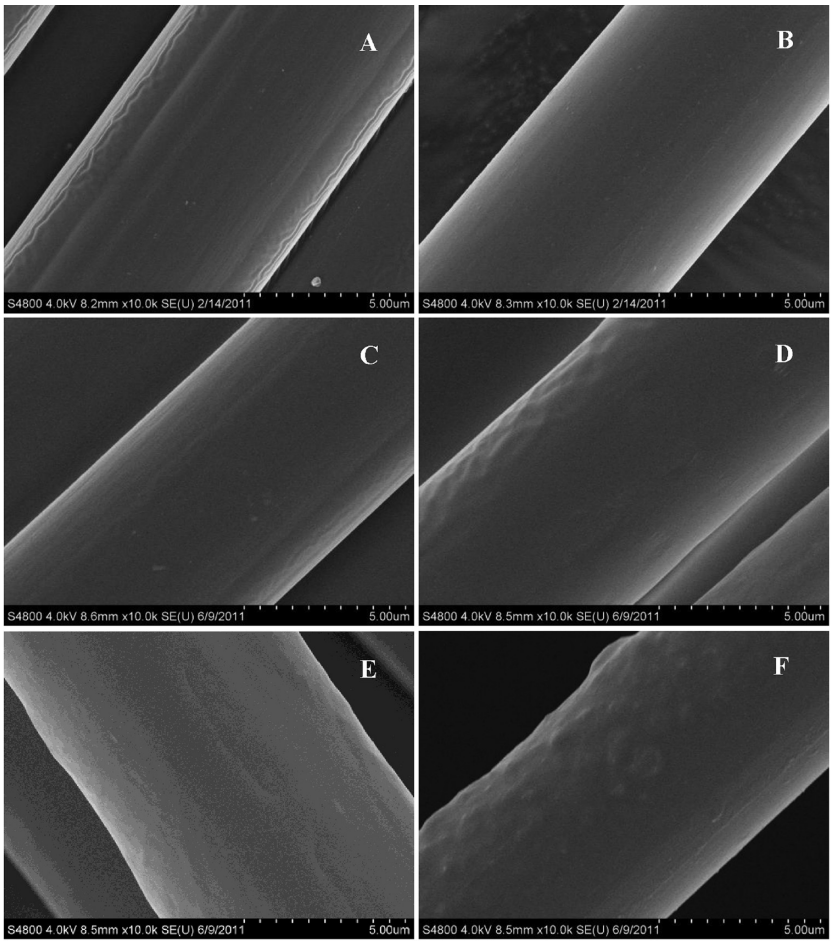

Figure 3. Scanning electron microscopy (SEM) images of the carbon fibers after GO modified sizing treatment: (A) T700S; (B) virgin carbon fiber (CF); (C) SCF-GO0; (D) SCF-GO1; (E) SCF-GO5; (F) SCF-GO10.

graphene oxide sheets.[22−24] This observation leads to a conclusion that complete exfoliation of graphite oxide down to individual graphene oxide sheet was indeed achieved. Moreover, it was found that no precipitation was observed in the bottom of the bottle even after the dispersion of GO in water settled for three months at room temperature (the digital photograph of aqueous GO dispersion is shown in Figure S1, see the Supporting Information). This result suggested that the resulting GO sheets could be well-dispersed into aqueous media forming homogeneous dispersions with good stability. These stable GO dispersions can be used for the preparation of modified sizing, which will facilitate the production of emulsion sizing agent for further manufacture of modified carbon fibers.

3.2. Surface Topography of Modified Carbon Fibers. The surface topography's changes for the carbon fibers after different sizing agent treatment were verified by the SEM, and the results are shown in Figure 3. Table 1 shows the abbreviations used for these material systems. Wrinkles along the fiber axis can be seen on the surface of commercial fiber T700S (Figure 3A). After removing the commercial sizing, the virgin carbon fiber with smooth surface was observed (Figure 3B). Figure 3C−F shows the surface topographies of carbon fiber after being treated by sizing agent with varied content of GO. The surfaces of modified carbon fibers are all uniform, and the sizing resin thickness of the modified carbon fibers is 0.2−0.5 μm, which was determined by SEM photographs according to the diameter difference between the virgin carbon fibers (the diameter is 6.8 μm, with standard deviation smaller than 0.05 μm) and GO-modified carbon fibers (the diameter is 7.2−7.8 μm). Furthermore, the GO content appears to have an obvious effect on the external fiber surface. Contrasting the GO-modified carbon fibers to the SCF-GO0, it can be found that the surfaces of SCF-GO1 and SCF-GO5 have some slight

Table 1. Abbreviations Used for Various Samples Prepared

sample code	details
CF	desized T700S is named as virgin carbon fiber
SCF-GO0	virgin carbon fibers with commercial sizing (NEOXIL 965)
SCF-GO1	1 wt % GO-sized carbon fibers
SCF-GO2.5	2.5 wt % GO-sized carbon fibers
SCF-GO5	5 wt % GO-sized carbon fibers
SCF-GO7.5	7.5 wt % GO-sized carbon fibers
SCF-GO10	10 wt % GO-sized carbon fibers
SCF-GO0-EP	commercial-sized carbon fiber-reinforced composites with neat epoxy matrix
SCF-GO1-EP	1 wt % GO-sized carbon fiber-reinforced composites with neat epoxy matrix
SCF-GO2.5-EP	2.5 wt % GO-sized carbon fiber-reinforced composites with neat epoxy matrix
SCF-GO5-EP	5 wt % GO-sized carbon fiber-reinforced composites with neat epoxy matrix
SCF-GO7.5-EP	7.5 wt % GO-sized carbon fiber-reinforced composites with neat epoxy matrix
SCF-GO10-EP	10 wt % GO-sized carbon fiber-reinforced composites with neat epoxy matrix

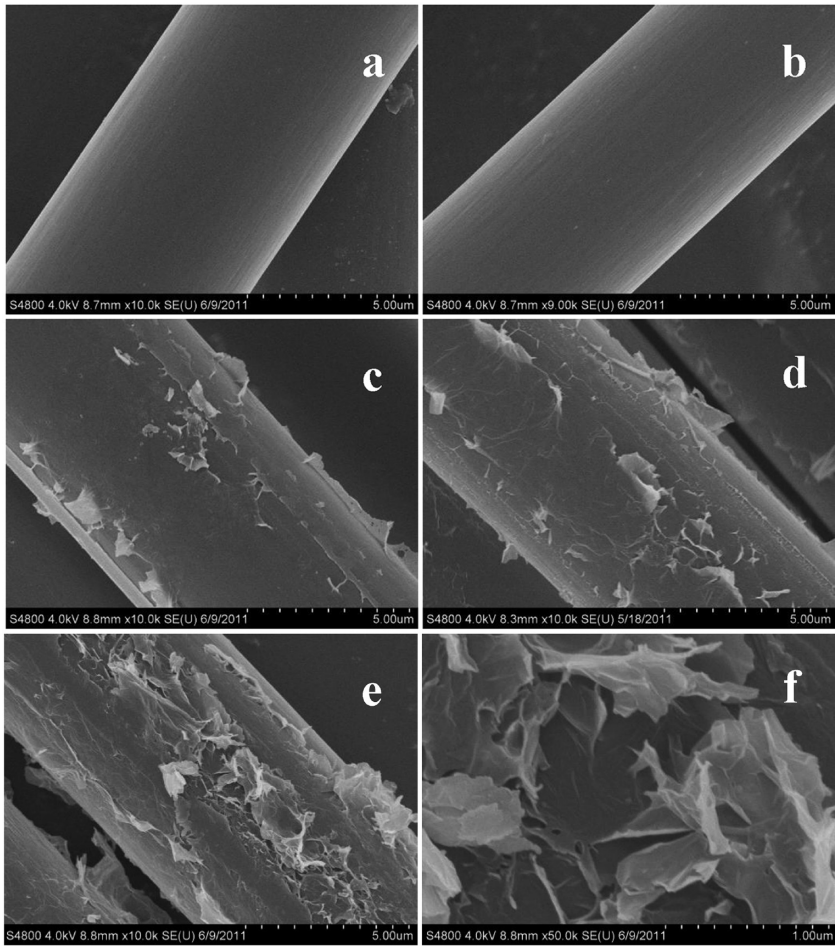

Figure 4. Scanning electron microscopy (SEM) images of the carbon fibers after thermal defunctionalization (800 °C, N_2): (a) virgin carbon fiber (CF); (b) SCF-GO0; (c) SCF-GO1; (d) SCF-GO5; (e) SCF-GO10; (f) the dashed circle area in image e with higher magnification.

concave pits and convex hills, whereas the surface of SCF-GO10 has much more convex hills, which means that the surface roughness of carbon fiber increases with increasing GO content in the sizing agent. The concave pits and convex hills on the surface of fiber, which may be caused by the randomly dispersed graphene oxide sheets in the sizing resin. To conclusively demonstrate this hypothesis, it is necessary to observe the distribution of GO sheets in these interfacial regions. However, it is difficult to directly observe the distribution of GO sheets in the interface region because of a significant amount of sizing resin on the fiber surface. Therefore, in the present work, thermal defunctionalization was used to remove the sizing resin before SEM analysis.

Figure 4 shows the SEM images of the carbon fibers after thermal defuctionalization. The randomly dispersed GO sheets on the surface of SCF-GO1, SCF-GO5, and SCF-GO10 have been clearly identified in Figure 4. One can see that a little content and uneven distribution of GO sheets on the surface of SCF-GO1, with the increase of the GO weight fraction from 1% to 5%, GO sheets can homogeneously cover the entire SCF-GO5 surface (Figure 4d), and it is more obviously as the weight fraction of GO increases to 10% (Figure 4e), whereas on the surface of SCF-GO10, some GO sheets agglomerates were also observed, as showm in Figure 4f, which might affect the degree of interfacial properties improvement. These images also reveal that GO sheets can be easily introduced to the interface regions of carbon fiber–resin matrix by modifying sizing agent formula, and the microstructure of the interfacial region varies with the content of GO sheets in the sizing agent.

3.3. Interfacial Shear Strength (IFSS). Interfacial shear strength (IFSS) results of each carbon fiber type can be seen in Figure 5, and the results are listed in Table 2. As shown in Figure 5, it is clearly demonstrated that the presence of GO

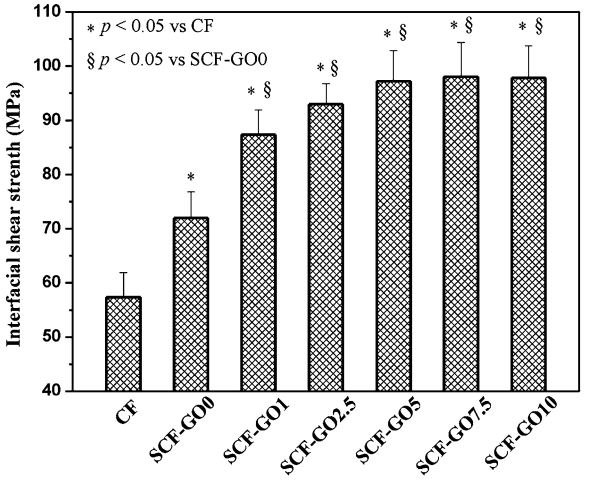

Figure 5. Interfacial shear strength (IFSS) results of single carbon fiber composites.

dx.doi.org/10.1021/am201757v | ACS Appl. Mater. Interfaces 2012, 4, 1543–1552

Table 2. Interfacial Shear Strength and Interlaminar Shear Strength (mean ± std deviation) for Different Materials (see Abbreviations in Table 1)

sample	IFSS (MPa)	increase (%)[a] (a)	(b)	sample	ILSS (MPa)	increase (%)[a] (c)
CF	57.4 ± 4.5					
SCF-GO0	72.0 ± 4.8	25.4		SCF-GO0-EP	45.5 ± 1.0	
SCF-GO1	87.4 ± 4.5	52.3	21.4	SCF-GO1-EP	46.0 ± 0.8	1.1
SCF-GO2.5	93.0 ± 3.8	62.0	29.2	SCF-GO2.5-EP	46.5 ± 0.8	2.2
SCF-GO5	97.2 ± 5.7	69.3	35.0	SCF-GO5-EP	51.3 ± 1.0	12.7
SCF-GO7.5	98.1 ± 6.3	70.9	36.3	SCF-GO7.5-EP	51.0 ± 0.7	12.1
SCF-GO10	97.9 ± 5.9	70.6	35.9	SCF-GO10-EP	50.7 ± 1.6	11.4

[a]"Increase (%)" calculation: CF as reference material for column (a); SCF-GO0 as reference material for column (b); SCF-GO0-EP as reference material for column (c).

sheets surrounding the fiber contributes to the improvement of the IFSS. The IFSS results of SCF-GO0, SCF-GO1, SCF-GO2.5, SCF-GO5, SCF-GO7.5, and SCF-GO10 fibers are 72.0, 87.4, 93.0, 97.2, 98.1, and 97.9 MPa, respectively. It is found that the IFSS of GO modified carbon fibers is much higher than that of commercial-sized carbon fiber, especially SCF-GO7.5 fiber yielding IFSS of 98.1 MPa, which has an increase of about 70.9% in comparison with CF fiber and about 36.3% in comparison with SCF-GO0 fiber. The advantages of this new method for interfacial enhancement can be demonstrated in contrast with the other parameter appeared in the literature.[8,13,25,26] For example, Yang et al.[8] reported a 39% improvement of IFSS for the 1 wt % nano-SiO_2-modified epoxy sizing treated carbon fiber in comparison with the unsized fibers.

The exact mechanisms of the improvement of IFSS are not clear, but it might be related to the increase of the wettability between fiber and matrix, the different interfacial microstructure, and chemical bonding between nanofillers and matrix resin after introducing the GO sheets into the interfacial region. As shown in Figure 3, it can be seen that the GO sheets surrounding the fiber surface are all covered by the sizing resin, and thus the surface energy of each type of sized fibers is the same, whereas the IFSS of GO sized fibers changes obviously. For the sized fibers, these results indicate that the wettability cannot be the main factor responsible for the improvement of interfacial shear strength. From the data in Table 2 and Figure 5, one can see that the IFSS may be highly dependent on the quantity and distribution of GO sheets in the interfacial region. When lower than 5 wt %, the GO sheets are well-dispersed in the sizing and homogeneously surrounding on the fiber surface, and the increase in loading causes significant improvements on the interfacial shear strength, whereas further increasing GO loading from 5 to 10 wt % leads to slight changes of IFSS. Herein, as shown in images e and f in Figure 4, it is noted that as further adding GO into sizing, the phenomenon of GO sheets agglomerate (or restacking together) occurs because of van der Waals force of the nano sheets. Rafiee et.al[27] reported that well-dispersion and homogeneous distribution of the GO sheets were highly effective in suppressing crack propagation in polymer matrix, and resulted in improving the strength and toughness of the polymer composites. Therefore, the agglomerated GO sheets which brought about local stress concentration and decreased the energy dissipation capability lead to less effective enhancement on the interfacial properties of the composites.[28] If the GO loading upon exceeding 10 wt %, it is anticipated that a significant amount of GO sheet will agglomerate in the interfacial regions and may become stress concentration sites resulting in deterioration of interfacial properties. Additionally, the GO sheets with many reactive groups,[29,30] including hydroxyl, epoxy, and carboxylic acid groups, were prepared successfully and verified by X-ray photoelectron spectroscopy (XPS) (XPS data are shown in Figure S2 in the Supporting Information). In the solidification procedure for carbon fiber/epoxy composites, amine hardener (the mixture of DDS and DDM) was used in this work. As GO contains reactive epoxy groups both on the basal planes and at the edges of sheets, its exposure to amine groups would lead to ring-opening reaction of the reactive three-membered epoxide ring, creating new C−N bonds.[6,31,32] Therefore, the curing agent not only solidified epoxy resin composites but also chemically connected GO sheets and epoxy component in the interfacial region through the reaction between epoxy groups of GO and amine units of the curing agent. In short, the chemically connected graphene oxide sheets were simultaneously obtained during the process of the solidification of the GO-modified carbon fiber composites. Besides, GO containing pendant oxygen-containing groups may form strong hydrogen bonds with the oxygen groups of epoxy resin. Therefore, it may lead to stronger interfacial interactions between GO sheets and epoxy resin in the interfacial region, and thus substantially larger enhancement of the properties of interface resin (modulus, strength, toughness).[6,33] So, the potential chemical reactions between epoxy and the GO sheets as well as hydrogen bonding might contribute to the improvement of the interfacial strength as well.

3.4. Interlaminar Shear Strength (ILSS). Interlaminar shear strength (ILSS) is one of the most important interfacial properties for composite. To better understand the relationship between the GO sheets surrounding the fiber and the interfacial properties, three-point short beam shear method was used to evaluate the interlaminar shear strength of the composites. In Figure 6 and Table 2, the ILSS values of the composites are presented. It is readily observed that higher than 2.5 wt % GO loading in the sizing made the sized fiber composites possess better ILSS compared with that of the commercial-sized fiber composites (SCF-GO0-EP). As shown in Figure 6, SCF-GO5-EP composite was measured to have a maximum interlaminar shear strength (51.3 MPa), with an increase of 12.7% as compared with SCF-GO0-EP composite, which is at a relatively high level of improvement for the hybrid reinforced composites in the literature.[34−36] However, the same as IFSS, a further increase in GO loading from 5 to 10 wt % leads to the slight changes of ILSS. These results are probably due to the homogenously dispersed GO sheets in the interfacial region of SCF-GO5-EP composite, which can serve as a supplementary

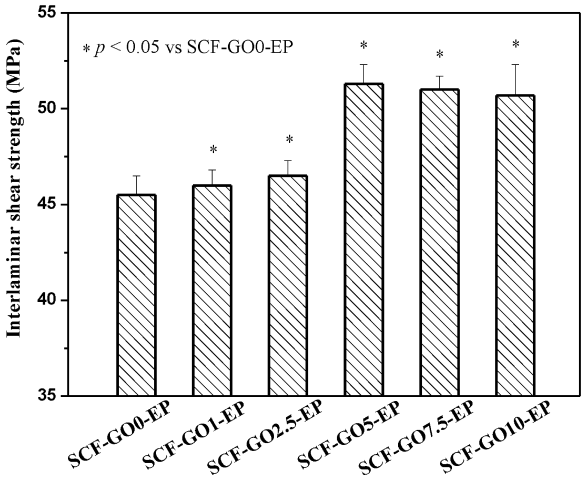

Figure 6. Interlaminar shear strength (ILSS) of unidirectional carbon fiber/epoxy composites.

reinforcement to the interface and further reduce the interlaminar stress concentration, enhance the strength and toughness of interfacial regions surrounding the fiber, and then finally result in improving the interlaminar shear strength.[37,38] But the excess of GO sheets results in a small amount of them agglomerated in the interfacial region of composites, such as the distribution of the GO sheets in the interfacial of SCF-GO10 as shown in images e and f in Figure 4, which probably reduced the interface toughness and strength because of influence of the stress distribution and interfacial fracture behavior of the interface layer,[39] and then accordingly weakened the interlaminar shear strength.

3.5. Micrographs of Fracture Surfaces. To help understand the interface behavior and enhancement mechanism of GO-modified carbon fiber/epoxy composites, we examined the fracture surfaces of unidirectional carbon fiber composites after short beam shear tests by scanning electron microscopy (SEM). SEM photomicrographs of fracture surfaces are shown in Figure 7 at two magnifications. As evident by the smooth and clean surfaces of the fibers (Figure 7A, B), the fracture micromechanism in SCF-GO0-EP and SCF-GO1-EP is seen to be primarily interfacial debonding. The SEM at a higher magnification (Figure 7A′, B′) clearly show the matrix completely detached from the fiber surface because of a weak adhesion. It indicates that the fiber/matrix debonding is the dominant mechanism of shear failure, and the weakest part of such composites is still the interface, even despite a small amount of GO sheets introducing into the interface region of SCF-GO1-EP composites. In comparison, for SCF-GO5-EP and SCF-GO10-EP composites, a significantly different interface microstructure is shown on the SEM micrographs (Figure 7C-D′). These composites do not display a complete matrix debonding from the fiber surface. A considerable plastic deformation and an amount of resin adhering to the carbon fiber surface can be seen on the fractographs (Figure 7C′ and D′). As an instance, in SCF-GO5-EP composite with 5 wt % GO sheets, a large number of needlelike and leaflike structures appear on the fracture surfaces, which facilitate the increase of the fractured surface area and degree of microcracking preceding the fracture. The development of these microstructures should be related to the interaction between the GO sheets and the matrix and seems to be responsible for the improvement of interlaminar shear strength. These results indicate that GO sheets cause the increasing strength and toughness of the interfacial region surrounding the carbon fiber. Therefore, the fracture failure occurs because of resin cracking and deformation within the matrix nearby the carbon fiber surface. However, some parts of the micrographs also show a combination of interfacial debonding in the fracture surface of SCF-GO5-EP and SCF-GO10-EP, which may be due to the lack of strong bonding between GO sheets and carbon fibers. So, a highly desirable stronger interfacial bonding between GO and carbon fiber may be necessary to obtain significant improvement of mechanical properties for carbon fiber composites.

3.6. Tensile Properties of UD Carbon Fiber Composites. To further inspect the enhancing effect of the GO-modified sizing, we investigated the tensile properties of unidirectional (UD) composites in accordance with ASTM standards. The results of tensile tests can be seen in Figure 8, and the detailed results are presented in Table S1 (see the Supporting Information). It is clearly verified in Figure 8 that the tensile strength of GO modified carbon fiber composites is greater than that of the commercial-sized fiber composites (SCF-GO0-EP). For tensile modulus of GO-modified composites, as shown in Figure 8, there are slight improvements observed in comparison with that of SCF-GO0-EP, showing a similar trend to the tensile strength. Tensile properties of UD fiber composites are in general dominated by the fiber behavior,[40] but it has been demonstrated that the tensile properties of fibers could be affected by altering the fiber surface nanostructures through introducing nanotubes/organoclays in fiber coating or surface.[10,11,41−43] Kim et al.[11] reported that both the tensile strength and the weibull modulus of the glass fiber composites coated with 0.5 wt % CNT−epoxy nanocomposite coating were higher than that of fiber composites coated with epoxy coating: a 13.7% increase in tensile stength and 45.8% increase in weibull modulus, respectively. They proposed that incorporation of CNTs in the epoxy further enhanced the effects of fiber coating on crack healing, which give rise to the improvement of tensile properties of the composites. In this study, the improvement of tensile performance of GO modified composites was also observed by introducing different content of GO sheets to the interfacial regions. Especially, the tensile strength of SCF-GO5-EP composites (1942.1 MPa) was 34.2% higher than that of SCF-GO0-EP (1446.7 MPa). However, a decrease was seen for GO-modified carbon fiber composites when the GO content increased to 7.5 and 10 wt % in sizing.

To better understand the role of GO modification in the improvement of the tensile properties, the fracture surfaces of composites were investigated by using SEM, as shown in Figure 9. For the commercial-sized carbon fiber composites (Figure 9A), it failed predominantly by progressive interfacial debonding and fiber pullout, followed by breakage of fibers at multilevels along the fiber direction. The pulled-out fibers of different lengths with a clean surface on the fracture surface indicated that the crack damage initiated from various locations along the interface, which demonstrated the weak interfacial bonding between the matrix and fiber. In contrast, GO-modified carbon fiber composites (Figure 9B, C) revealed the simultaneous breakage of fibers and matrix, the interfaces between the fiber and the matrix were almost intact even after failure, which evidenced strong interfacial bonding and led to higher tensile properties. Judging from the significant changes in the interfacial fracture morphology, it appears that the

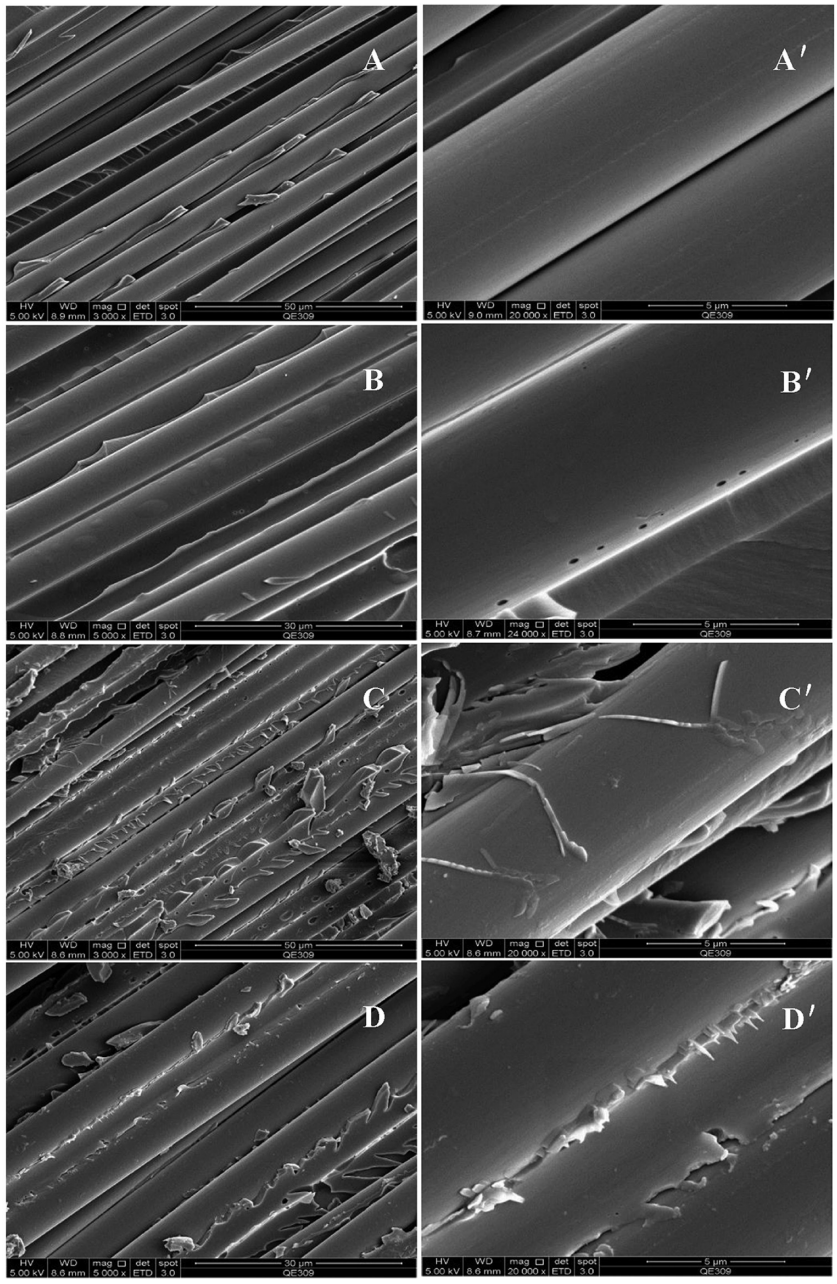

Figure 7. Fracture surface micrographs of carbon fiber/epoxy composites: (A, A′) SCF-GO0-EP; (B, B′) SCF-GO1-EP; (C, C′) SCF-GO5-EP; (D, D′) SCF-GO10-EP; (left) 50 μm scale bar magnification and (right) 5 μm scale bar magnification.

enhanced interface interactions are due to the presence of GO sheets in the sizing resin. As discussed above, GO sheets introduced to the interfacial regions of the fiber composites caused the increased strength and toughness of the interfacial region (a thin matrix) due to the "crack healing" effect and the potential chemical reactions between epoxy and GO sheets as well as hydrogen bonding. As a result, the strengthened interfacial region held the fiber and matrix together, which was mainly responsible for the transition in failure mode from interfacial debonding to transverse fracture. In addition, as shown in Figure 9, it was observed that the resin surrounding the fibers was still tightly attached to the fiber in SCF-GO5-EP, whereas minor delamination of fiber and matrix was verified in SCF-GO10-EP (SCF-GO7.5-EP, as shown in Figure 3S in the Supporting Information). These phenomena are probably attributed to the fact that the addition of GO sheets causes a randomly dispersion of particles within the regions surrounding fiber surface, which offers a strengthening mechanism by bridging the surface microcracks, as proposed in refs 9, 11, and 12. The "crack-tip bridging" effect promoted redistribution of the stresses around the surface cracks when 5 wt % GO sheets homogenously dispersed in the interfacial regions, thereby delaying the crack opening. However, further increased GO content in the sizing from 5 to 10 wt % was detrimental to the tensile properties of GO-modified carbon fiber composites, due to GO agglomeration in the interfacial region, which might have acted as a different type of stress concentration reducing the strength of interface. GO agglomerates in the specimen containing 10 wt % GO sheets were identified and discussed in section 3.3. In brief, the well-dispersed GO sheets give SCF-GO5-EP strong interfacial bonding between fibers and matrix

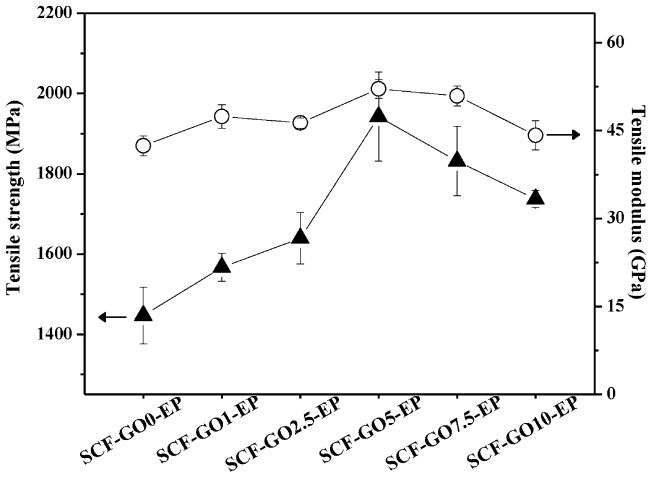

Figure 8. Tensile properties of unidirectional carbon fiber/epoxy composites tested in the fiber direction: Tensile strength (▲) and elastic modulus (○). $p < 0.05$ compared with SCF-GO0-EP.

which results in better tensile properties than the other composites.

4. CONCLUSIONS

In summary, the successfully exfoliated GO sheets can form a homogeneous and stable dispersion in aqueous media to further prepare stable GO-modified carbon fiber sizing. The GO sheets randomly dispersed surrounding the individual fiber surfaces by processing it with GO modified sizing agent. The IFSS of those composites could obtain about 70.9 and 36.3% improvement compared with that of the virgin carbon fiber composites and the commercial sizing modified carbon fiber composites, respectively. Furthermore, a 12.7% enhancement of ILSS was observed after introducing the GO sheets to the interfacial regions of carbon fibers and matrix compared with commercial-sizing-modified carbon fiber composites. The tensile properties of GO modified carbon fiber composites, including tensile strength and tensile modulus, are higher than that of the normal composites. Therefore, the presented approach will show potential for enhancing interfacial and tensile properties in carbon fiber-reinforced composites through using GO sheets modified fiber sizing.

■ ASSOCIATED CONTENT

Supporting Information

The digital photograph of aqueous dispersion of graphene oxide settled for 3 months. The X-ray photoelectron spectroscopy of graphene oxide in the C_{1s} region. The tensile properties results of UD carbon fiber composites. SEM images of fractured surfaces of UD carbon fiber composites. This material is available free of charge via the Internet at http://pubs.acs.org.

■ AUTHOR INFORMATION

Corresponding Author

*Fax: +86-574-86685802. E-mail: xinyu.fan@nimte.ac.cn.

Notes

The authors declare no competing financial interest.

■ ACKNOWLEDGMENTS

This work was financially supported by Knowledge Innovation Program of the Chinese Academy of Sciences (KGCX2-EW-210), Ningbo Natural Science Foundation (2011A610115 and 2011A610113), Ningbo Postdoctoral Special Financial Support (2011-327), Zhejiang Provincial Natural Science Foundation (Y4110609) and National Natural Science Foundation of China (51103173).

■ REFERENCES

(1) Argon, A. S.; Cohen, R. E. *Polymer* **2003**, *44*, 6013−6032.
(2) Garg, A. C.; Mai, Y. W. *Compos. Sci. Technol.* **1988**, *31*, 179−223.
(3) Rafiee, M. A.; Rafiee, J.; Wang, Z.; Song, H. H.; Yu, Z. Z.; Koratkar, N. *Acs Nano* **2009**, *3*, 3884−3890.
(4) Yang, H. F.; Li, F. H.; Shan, C. S.; Han, D. X.; Zhang, Q. X.; Niu, L.; Ivaska, A. *J. Mater. Chem.* **2009**, *19*, 4632−4638.

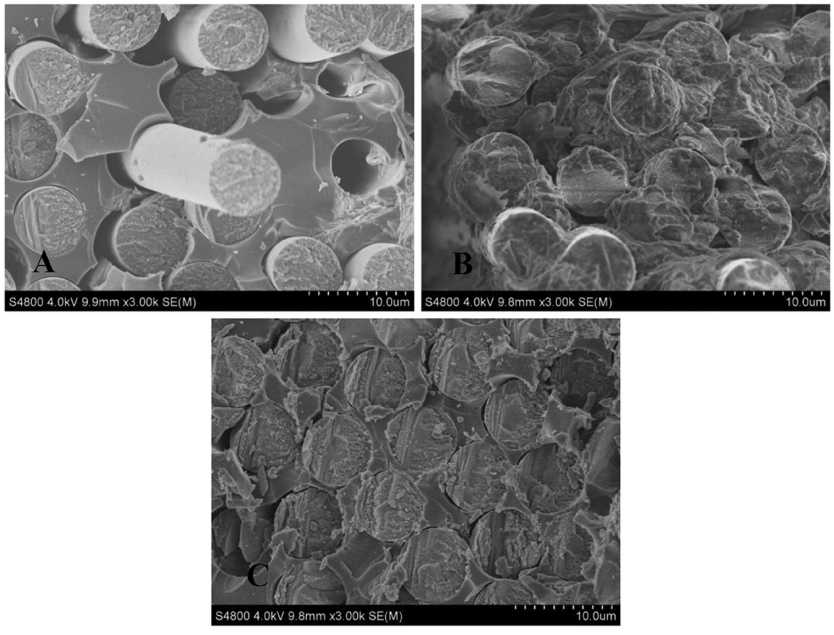

Figure 9. SEM images of fractured surfaces of UD carbon fiber composites: (A) SCF-GO0-EP; (B) SCF-GO5-EP; (C) SCF-GO10-EP.

(5) Kulkarni, D. D.; Choi, I.; Singamaneni, S.; Tsukruk, V. V. *ACS Nano* **2010**, *4*, 4667−4676.
(6) Yang, H. F.; Shan, C. S.; Li, F. H.; Zhang, Q. X.; Han, D. X.; Niu, L. *J. Mater. Chem.* **2009**, *19*, 8856−8860.
(7) Yavari, F.; Rafiee, M. A.; Rafiee, J.; Yu, Z. Z.; Koratkar, N. *ACS Appl. Mater. Interfaces* **2010**, *2*, 2738−2743.
(8) Yang, Y.; Lu, C. X.; Su, X. L.; Wang, X. K. *J. Mater. Sci.* **2007**, *42*, 6347−6352.
(9) Gao, S. L.; Mader, E.; Plonka, R. *Acta Mater.* **2007**, *55*, 1043−1052.
(10) Siddiqui, N. A.; Li, E. L.; Sham, M. L.; Tang, B. Z.; Gao, S. L.; Mader, E.; Kim, J. K. *Compos. Part: A-Appl. S* **2010**, *41*, 539−548.
(11) Siddiqui, N. A.; Sham, M. L.; Tang, B. Z.; Munir, A.; Kim, J. K. *Compos. Part: A-Appl. S* **2009**, *40*, 1606−1614.
(12) Gao, S. L.; Mader, E.; Plonka, R. *Compos. Sci. Technol.* **2008**, *68*, 2892−2901.
(13) Godara, A.; Gorbatikh, L.; Kalinka, G.; Warrier, A.; Rochez, O.; Mezzo, L.; Luizi, F.; VanVuure, A. W.; Lomov, S. V.; Verpoest, I. *Compos. Sci. Technol.* **2010**, *70*, 1346−1352.
(14) Warrier, A.; Godara, A.; Rochez, O.; Mezzo, L.; Luizi, F.; Gorbatikh, L.; Lomov, S. V.; VanVuure, A. W.; Verpoest, I. *Compos., Part A* **2010**, *41*, 532−538.
(15) Drown, E. K.; Almoussawi, H.; Drzal, L. T. *J. Adhes. Sci. Technol.* **1991**, *5*, 865−881.
(16) Tang, L. G.; Kardos, J. L. *Polym. Compos.* **1997**, *18*, 100−113.
(17) Gonon, L.; Momtaz, A.; Vanhoyweghen, D.; Chabert, B.; Gerard, J. F.; Gaertner, R. *Polym. Compos.* **1996**, *17*, 265−274.
(18) Stankovich, S.; Piner, R. D.; Nguyen, S. T.; Ruoff, R. S. *Carbon* **2006**, *44*, 3342−3347.
(19) Stankovich, S.; Piner, R. D.; Chen, X. Q.; Wu, N. Q.; Nguyen, S. T.; Ruoff, R. S. *J. Mater. Chem.* **2006**, *16*, 155−158.
(20) Miller, B.; Muri, P.; Rebenfeld, L. *Compos. Sci. Technol.* **1987**, *28*, 17−32.
(21) *ASTM D2344: Standard test method for apparent interlaminar shear strength of parallel fiber composites by short-beam method*; American Society for Testing and Materials: Philadelphia, PA, 1984.
(22) Stankovich, S.; Dikin, D. A.; Piner, R. D.; Kohlhaas, K. A.; Kleinhammes, A.; Jia, Y.; Wu, Y.; Nguyen, S. T.; Ruoff, R. S. *Carbon* **2007**, *45*, 1558−1565.
(23) Stankovich, S.; Dikin, D. A.; Dommett, G. H. B.; Kohlhaas, K. M.; Zimney, E. J.; Stach, E. A.; Piner, R. D.; Nguyen, S. T.; Ruoff, R. S. *Nature* **2006**, *442*, 282−286.
(24) Gomez-Navarro, C.; Burghard, M.; Kern, K. *Nano Lett.* **2008**, *8*, 2045−2049.
(25) Qian, H.; Bismarck, A.; Greenhalgh, E. S.; Kalinka, G.; Shaffer, M. S. P. *Chem. Mater.* **2008**, *20*, 1862−1869.
(26) Schaefer, J. D.; Rodriguez, A. J.; Guzman, M. E.; Lim, C. S.; Minaie, B. *Carbon* **2011**, *49*, 2750−2759.
(27) Rafiee, M. A.; Rafiee, J.; Srivastava, I.; Wang, Z.; Song, H. H.; Yu, Z. Z.; Koratkar, N. *Small* **2010**, *6*, 179−183.
(28) Rafiq, R.; Cai, D. Y.; Jin, J.; Song, M. *Carbon* **2010**, *48*, 4309−4314.
(29) Cai, W.; Piner, R. D.; Stadermann, F. J.; Park, S.; Shaibat, M. A.; Ishii, Y.; Yang, D.; Velamakanni, A.; An, S. J.; Stoller, M.; An, J.; Chen, D.; Ruoff, R. S. *Science* **2008**, *321*, 1815−1817.
(30) Stankovich, S.; Piner, R. D.; Chen, X. Q.; Wu, N. Q.; Nguyen, S. T.; Ruoff, R. S. *J. Mater. Chem.* **2006**, *16*, 155−158.
(31) Wang, S.; Chia, P. J.; Chua, L. L.; Zhao, L. H.; Png, R. Q.; Sivaramakrishnan, S.; Zhou, M.; Goh, R. G. S.; Friend, R. H.; Wee, A. T. S.; Ho, P. K. H. *Adv. Mater.* **2008**, *20*, 3440−3446.
(32) Morrison, R. T.; Boyd, R. N. *Organic Chemistry*, 6th ed.; Prentice-Hall: Upper Saddle River, NJ, 1992.
(33) Xu, Y. X.; Hong, W. J.; Bai, H.; Li, C.; Shi, G. Q. *Carbon* **2009**, *47*, 3538−3543.
(34) Lee, S. B.; Choi, O.; Lee, W.; Yi, J. W.; Kim, B. S.; Byun, J. H.; Yoon, M. K.; Fong, H.; Thostenson, E. T.; Chou, T. W. *Compos., Part A* **2011**, *42*, 337−344.
(35) Yang, Y.; Lu, C. X.; Su, X. L.; Wu, G. P.; Wang, X. K. *Mater. Lett.* **2007**, *61*, 3601−3604.
(36) Rodriguez, A. J.; Guzman, M. E.; Lim, C. S.; Minaie, B. *Carbon* **2011**, *49*, 937−948.
(37) Zhu, J.; Imam, A.; Crane, R.; Lozano, K.; Khabashesku, V. N.; Barrera, E. V. *Compos. Sci. Technol.* **2007**, *67*, 1509−1517.
(38) Schwartz, H. S.; Hartness, J. T. Effect of fiber coating on interlaminar fracture. toughness of composites. In *Toughened Composites*. Johnston, N. J., Ed.; American Society for Testing and Materials: Philadelphia, PA, 1987; ASTM STP 937, Vol.5, pp 150−178.
(39) Ajayan PM, S. L.; Braun, P. V. *Nanocomposite Science and Technology*; Wiley-VCH: Weinheim, Germany, 2003; Vol.3, p 138.
(40) Godara, A.; Mezzo, L.; Luizi, F.; Warrier, A.; Lomov, S. V.; Vuure, A. W.; Gorbatikh, L.; Moldenaers, P.; Verpoest, I. *Carbon* **2009**, *47*, 2914−2923.
(41) Zhao, F.; Huang, Y. D.; Liu, L.; Bai, Y. P.; Xu, L. W. *Carbon* **2011**, *49*, 2624−2632.
(42) Guo, J. H.; Lu, C. X.; An, F. *J. Mater. Sci.* **2012**, *47*, 2831−2836.
(43) An, F.; Lu, C. X.; Guo, J. H.; He, S. Q.; Lu, H. B.; Yang, Y. *Appl. Surf. Sci.* **2011**, *258*, 1069−1076.